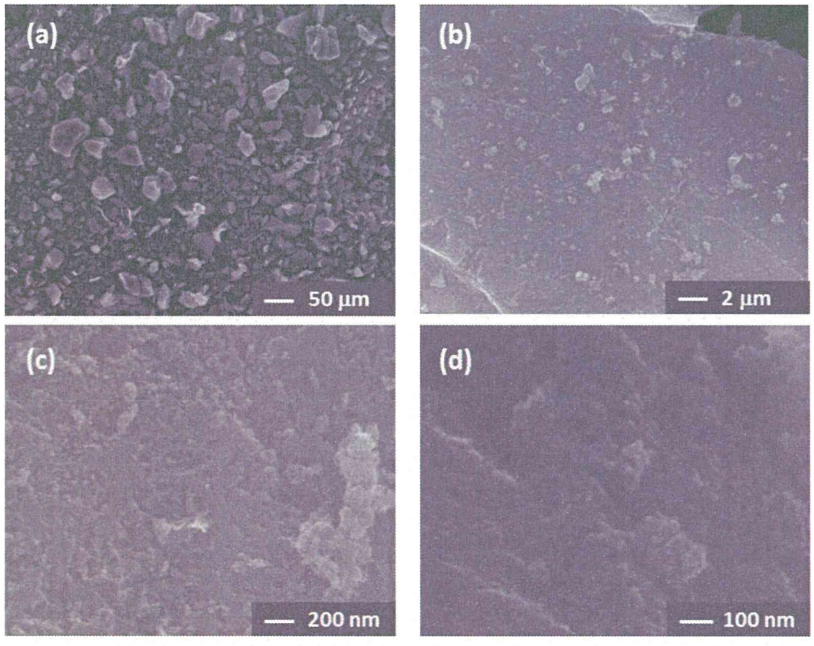

Figure 5. FE-SEM images of AC (a) × 200, (b) × 5,000, (c) × 50,000, and (d) × 100,000.

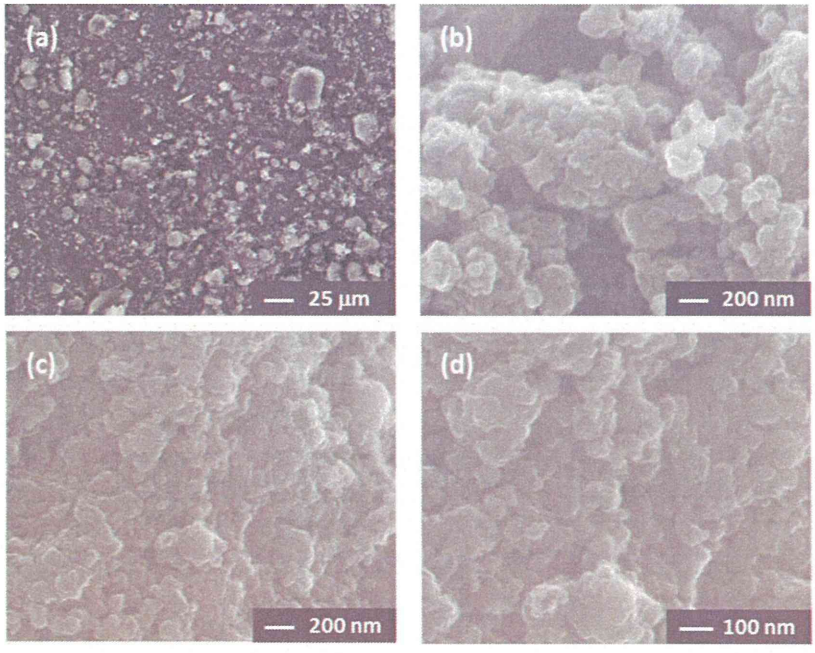

Figure 6. FE-SEM images of HFS1 (a) × 400, (b) × 50,000, (c) × 50,000, and (d) × 100,000.

ability, using this method. The antioxidant activities were determined as %AOA values defined by the following equation (1):

$$\%\mathrm{AOA} = \frac{[(k_{\mathrm{obs}}\ \text{of control}) - (k_{\mathrm{obs}}\text{of sample})}{k_{\mathrm{obs}}\ \text{of control}} \times 100 \qquad (1)$$

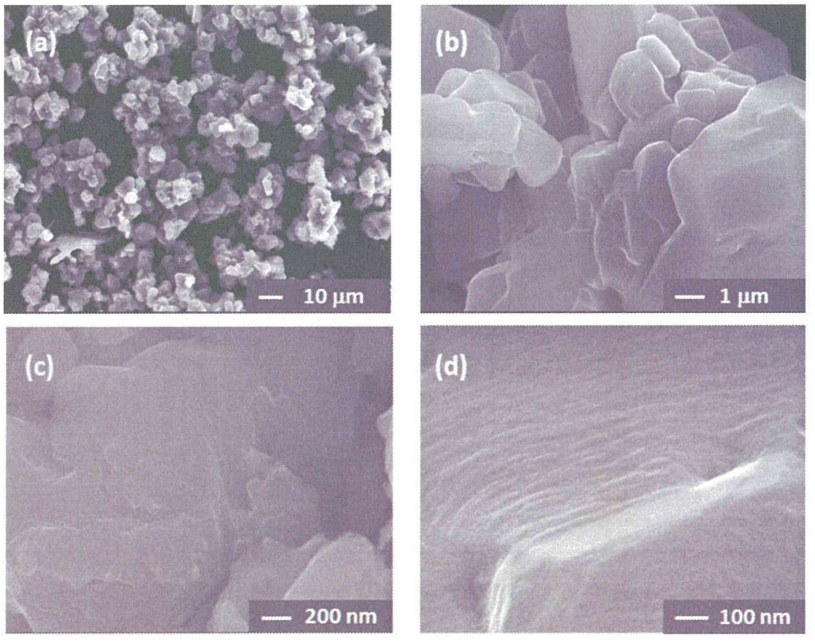

Figure 7. FE-SEM images of C_{60} (a) × 800, (b) × 10,000, (c) × 50,000, and (d) × 100,000.

where k_{obs} is the rate constant of β-carotene bleaching in the absence (control) or presence of fullerenes.

The reaction of β-carotene with linoleic acid solubilized with the surfactant Tween 40 in buffer solution under air at 50°C in the absence and presence of HFS1 and HFS2 as antioxidants were monitored by a UV-vis spectrometer equipped with a thermo-controller and a magnetic stirrer by measuring the absorbance at 460 nm (Figure 8) (27). By addition of HFSs, the discoloration of β-carotene by radical attack was clearly suppressed. The plots of $\ln[(Abs_0)/(Abs_t)]$ versus reaction time gave a linear regression line for each curve, proving the pseudo first-order decay of β-carotene k_{obs}. The measurement was repeated at least three times for each sample to evaluate its reproducibility with the value of standard deviation for k_{obs} (Table 2).

Table 2
Bleaching rate constant k_{obs} and %AOA values of various antioxidants (10 μM)

Antioxidants	$10^4 k_{obs}$ / s^{-1}	%AOA
none (control)	7.44 ± 0.89	0
catechin (positive control)	1.47 ± 0.15	80.2
C_{60}/PVP[a]	3.76 ± 0.14	49.5
$C_{60}(OH)_{36}$	3.45 ± 0.30	53.6
HFS1[b]	0.987 ± 0.079	86.7
HFS2[b]	1.92 ± 0.18	74.2

[a]Polyvinylpyrrolidone (PVP)-entrapped C_{60} as a water-soluble fullerene was used.
[b]The similar mass concentration as $C_{60}(OH)_{36}\bullet 8H_2O$ was used (0.004wt%).

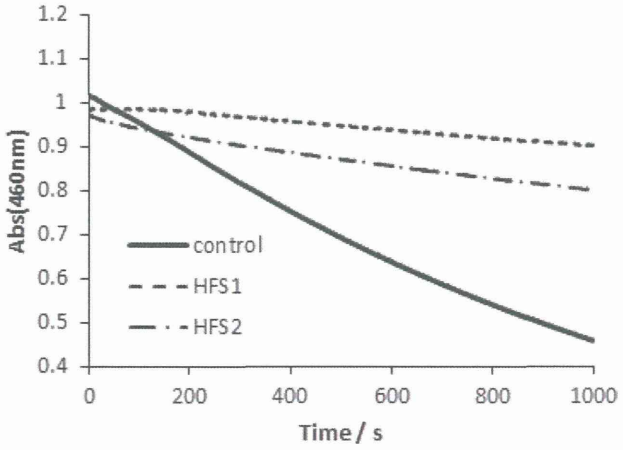

Figure 8. Time course of β-carotene bleaching assay monitoring absorbance at 460 nm at 50°C in the absence (control) and presence of antioxidants (HFS1 and HFS2).

The %AOA values of various antioxidants tested are summarized in Table 2. Consistent with the high reactivity of fullerenes toward radical species, fullerenol $C_{60}(OH)_{36}$ had a moderately high %AOA of 53.6% compared with that of the reference C_{60}/PVP (49.5%). Interestingly, hydrophilic FS exhibited a much higher %AOA, at 86.7% and 74.2% for HFS1 and HFS2, than the fullerenes. The antioxidant activity of FS has not previously been reported, and thus the present less expensive and easily available hydrophilic FS will give a great promise for applications in numerous fields as a novel radical scavenging antioxidant.

3.3. Possible Reaction Mechanism

A plausible reaction mechanism for the polyhydroxylation of C_{60} using hydrogen peroxide to give $C_{60}(OH)_{36/44}$ is illustrated in Scheme 2. The $^{-}$OOH (or •OH via the radical path) formed from H_2O_2 in equilibrium with $^{-}$OH from tetra-*n*-butyl ammonium hydroxide (TBAH) attacks C_{60} to initially afford fullerene oxide $C_{60}O$, followed by the attack of $^{-}$OH and protonation. The epoxidation process may be repeated to give $C_{60}O_2$, $C_{60}O_3$, and so on, which are more susceptible than $C_{60}O$ to the subsequent nucleophilic attack of $^{-}$OH (or $^{-}$OOH) because of the higher strain. These fullerene oxide intermediates were clearly detected in the reaction mixture by liquid chromatography-mass spectrometry (LC-MS; APCI; $m/z = 736$, 752, and 768) and were proven to be the intermediates by their kinetic behavior. Carbon nanotubes can also be oxidized using hydrogen peroxide (22), although only the edge carbons of nanotubes can be modified, and carboxyl groups are introduced instead of hydroxyl groups. The oxidation mechanism of soot is unclear at present; however, the results of elemental analysis, particle size analysis, and antioxidant activity imply that a mechanism similar to that of fullerene may be involved.

4. Conclusion

The polyhydroxylation method for C_{60} using hydrogen peroxide was applied to fullerene soot (FS) to yield the corresponding hydrophilic fullerene soot (HFS). The IR and elemental analysis indicated the successful introduction of oxygen-containing groups. Particle size

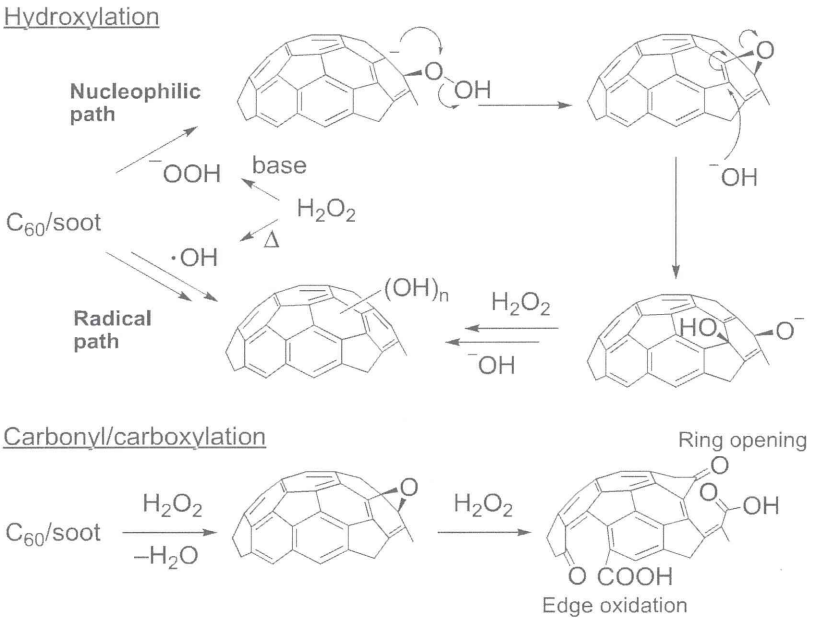

Scheme 2. Plausible mechanisms for the polyhydroxylation and oxidation of C_{60}/soot using H_2O_2.

analysis revealed relatively high dispersion property of HFS in water with particle size of 70–200 nm. The FE-SEM observation represented the particle-aggregated fine structure of FS and its negligible morphology change by hydrophilic treatment with H_2O_2. Hydrophilic fullerene soot exhibited high antioxidant activity (%AOA), high radical scavenging ability, as evaluated by β-carotene bleaching assay up to 87% for HFS1 compared with fullerenol $C_{60}(OH)_{36}$ (54%) and C_{60} (50%).

Acknowledgments

This work was partially supported by a Grant-in-Aid for Scientific Research No. 23651111 from the MEXT, Japan and by Health Labor Sciences Research Grants from the Ministry of Health, Labor, and Welfare of Japan (MHLW).

References

1. Kokubo, K. (2012) In *The Delivery of Nanoparticles*; Hashim, A.A. (ed.), InTech: Croatia, pp. 317–332.
2. Nakashima, N. (2005) *Int. J. Nanosci.*, 4: 119–137.
3. Osawa, E. (2010) In *Chemistry of Nanocarbons*; Akasaka, T., Wudl, F., and Nagase, S. (eds.), John Wiley & Sons: New York, pp. 413–432.
4. Chiang, L.Y., Wang, L.-Y., Swirczewski, J.W., Soled, S., and Cameron, S. (1994) *J. Org. Chem.*, 59: 3960–3968.
5. Li, J., Takeuchi, A., Ozawa, M., Li, X., Saigo, K., and Kitazawa, K. (1993) *J. Chem. Soc., Chem. Commun.*, 1784–1785.
6. Kokubo, K., Matsubayashi, K., Tategaki, H., Takada, H., and Oshima, T. (2008) *ACS Nano*, 2: 327–333.

7. Kokubo, K., Shirakawa, S., Kobayashi, N., Aoshima, H., and Oshima, T. (2011) *Nano Res.*, 4: 204–215.
8. Akasaka, T. and Nagase, S. (2002) *Endofullerenes: A New Family of Carbon Clusters*, Kluwer: Dordrecht, The Netherlands.
9. Mikawa, M., Kato, H., Okumura, M., Narazaki, M., Kanazawa, Y., Miwa, N., and Shinohara, H. (2001) *Bioconjugate Chem.*, 12: 510–514.
10. Sitharaman, B., Bolskar, R. B., Rusakova, I., and Wilson, L. J. (2004) *Nano Lett.*, 4: 2373–2378.
11. Ueno, H., Nakamura, Y., Ikuma, N., Kokubo, K., and Oshima, T. (2012) *Nano Res.*, 5: 558–564.
12. Ueno, H., Kokubo, K., Kwon, E., Nakamura, Y., Ikuma, N., and Oshima, T. (2013) *Nanoscale*, 5: 2317–2321.
13. Saitoh, Y., Xiao, L., Mizuno, H., Kato, S., Aoshima, H., Taira, H., Kokubo, K., and Miwa, N. (2010) *Free Radic. Res.*, 44: 1072–1081.
14. Saitoh, Y., Mizuno, H., Xiao, L., Hyoudou, S., Kokubo, K., and Miwa, N. (2012) *Mol. Cell. Biochem.*, 366: 191–200.
15. Aoshima, H., Kokubo, K., Shirakawa, S., Ito, M., Yamana, S., and Oshima, T. (2009) *Biocont. Sci.*, 14: 69–72.
16. Saitoh, Y., Miyanishi, A., Mizuno, H., Kato, S., Aoshima, H., Kokubo, K., and Miwa, N. (2011) *J. Photochem. Photobiol. B*, 102: 69–76.
17. Inui, S., Aoshima, H., Ito, M., Kokubo, K., and Itami, S. (2012) *J. Cosmet. Sci.*, 63: 259–268.
18. Maeda, Y., Kato, T., Higo, J., Hasegawa, T., Kitano, T., Tsuchiya, T., Akasaka, T., Okazaki, T., Lu, J., and Nagase, S. (2008) *Nano*, 4: 455–459.
19. Takaya, Y., Kishida, H., Hayashi, T., Michihata, M., and Kokubo, K. (2011) *CIRP Ann. –Manuf. Techn.*, 60: 567–570.
20. Saotome, T., Kokubo, K., Shirakawa, S., Oshima, T., and Hahn, H.T. (2011) *J. Compos. Mater.*, 45: 2595–2601.
21. Raebiger, J.W., Alford, J.M., Bolskar, R.D., and Diener, M.D. (2011) *Carbon*, 49: 37–46.
22. Kasai, R., Yaegashi, H., Yokoyama, H., Yamanaka, M., and Sawada, H. (2007) *J. Mater. Sci.*, 42: 10228–10238.
23. Miyata, Y., Maniwa, Y., and Kataura, H. (2006) *J. Phys. Chem. B*, 110: 25–29.
24. Karousis, N., Tagmatarchis, N., and Tasis, D. (2010) *Chem. Rev.*, 110: 5366–5397.
25. Rafiq, R., Cai, D., Jin, J., and Song, M. (2010) *Carbon*, 48: 4309–4314.
26. Veerapandian, M., Lee, M.-H., Krishnamoorthy, K., and Yun, K. (2012) *Carbon*, 50: 4228–4238.
27. Takada, H., Kokubo, K., Matsubayashi, K., and Oshima, T. (2006) *Biosci. Biotechnol. Biochem.*, 70: 3088–3093.

ChemComm

COMMUNICATION

View Article Online
View Journal | View Issue

First synthesis and aggregation behaviour of periconjugated triazoliumfullerene†

Cite this: *Chem. Commun.*, 2014, 50, 581

Received 29th July 2013,
Accepted 20th October 2013

DOI: 10.1039/c3cc45783d

www.rsc.org/chemcomm

Naohiko Ikuma,* Saori Inaba, Ken Kokubo and Takumi Oshima

Triazoliumfullerene was first prepared by the [3+2] cycloaddition of *in situ* generated 1,3-diaza-2-azoniaallene with fullerene and was characterized by the dispersed positive charge over the fullerene sphere associated with periconjugation. This new type of amphiphilic fullerene tended to form vesicles and crystalline aggregates after the casting of THF or MeOH solutions.

Ionic fullerenes[1–6] are useful compounds for medical applications such as in antibacterial[1f] and anti-HIV[1g] agents, and also for self-assembling nanocarbon materials[2,3] owing to the presence of amphiphilic intermolecular ionic, dipole–dipole, π–π and hydrophobic interactions. These ionic and highly polar fullerenes are apt to form vesicle,[1h,2,3] nanowire,[1h,2,4] and nanosheet[5] structures by way of self-assembly. Their aggregation behaviors highly depend on how the introduced ionic (hydrophilic) groups electronically affect the nonpolar (hydrophobic) fullerene cage. Here, it is interesting to know what kind of aggregation occurs if the ionic charge is dispersed on the π-conjugated fullerene cage. Such charge dispersion can be attained for the nitrogen incorporated 60π ionic azafullerene ($C_{59}N^+$).[6] However, the extremely low stability and intrinsic activity of reduction[7] restricted its usual application as an ionic fullerene.

This situation prompted us to design a new type of ionic fullerene with possible conjugation; one promising candidate is through-space periconjugation[8] between the outer ionic site and the π-conjugated fullerene cage. We have attempted the introduction of a cationic 1,2,3-triazolium unit[9] into the fullerene sphere, because the possible high delocalization of positive charge on the N_1–N_2–N_3 linkage will allow direct electron withdrawal as well as possible periconjugation with the adjacent fullerene *cis*-1 π-orbital. By DFT calculations,[10] it was found that the LUMO of the triazoliumfullerene was delocalized both on the cationic N_1–N_2–N_3 linkage and the fullerene cage (Fig. 1a and b), and the LUMO level was 0.36 eV lower than that of pyrrolidiniumfullerene (Fig. 1d and e),[1a–d,2,5a] a typical ammonium fullerene. Moreover, in the electrostatic potential (ESP) map of pyrrolidiniumfullerene, the positive site is apparently localized on the pyrrolidinium moiety (blue on the ESP map in Fig. 1f) and the fullerene sphere remains in a less charged state. By contrast, the ESP map of triazoliumfullerene shows a considerable distribution of positive charge over the fullerene cage with an ambiguous boundary (Fig. 1c), whereby its dipole moment is smaller than that of pyrrolidiniumfullerene. Therefore, triazoliumfullerene (as a salt) is expected to behave as a unique amphiphile in contrast to the previously employed ionic fullerenes. In this communication,

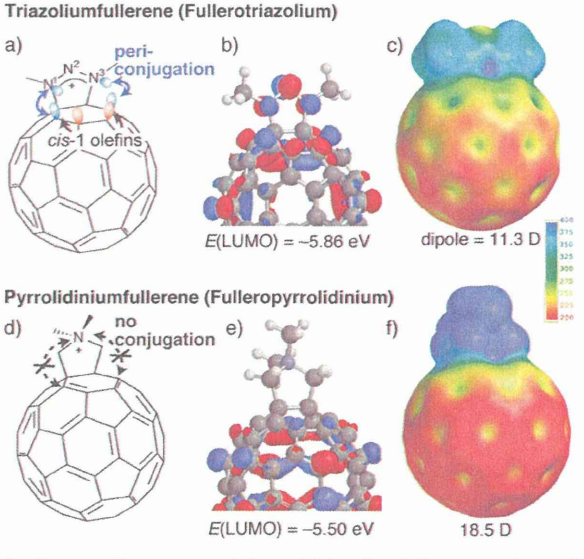

Fig. 1 Comparative representation of triazoliumfullerene and pyrrolidiniumfullerene: (a,d) molecular structure, (b,e) LUMO with its levels shown, (c,f) electrostatic potential (ESP) maps of the electron density contours and dipole moments with a color bar of ESP energy (kJ mol^{-1}); *i.e.*, blue is more electropositive (cationic) while red is lower (relatively apolar). DFT calculations were carried out with the B3LYP/6-31G(d) level of theory.

Division of Applied Chemistry, Graduate School of Engineering, Osaka University, Suita, Osaka 565-0871, Japan. E-mail: ikuma@chem.eng.osaka-u.ac.jp

† Electronic supplementary information (ESI) available: Synthesis, $^1H/^{13}C$ NMR charts (with DFT simulation) and magnified SEM/TEM images of 3^+, and calculated TS coordinates. See DOI: 10.1039/c3cc45783d

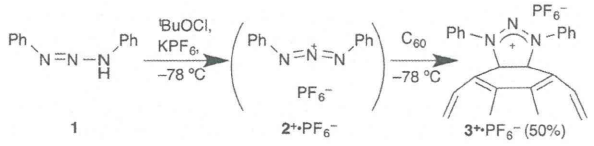

Scheme 1

we report the one-pot first synthesis of triazoliumfullerene (as a PF_6 salt), theoretical calculation of the mechanistic pathway, and preliminary DLS/SEM/TEM measurements of its self-aggregation.

To prepare triazoliumfullerene, we employed [3+2] cycloaddition[9] of 1,3-diaza-2-azoniaallene salt 2^+ with fullerene as a 2π component. The intermediate 2^+ was generated *in situ via* sequential chlorination and ionization of commercially available diphenyltriazene **1** by *tert*-butyl hypochlorite and the Lewis acid KPF_6[11] at −78 °C. To avoid spontaneous decomposition of the unstable intermediate 2^+, a one-pot reaction was carried out with C_{60} at −78 °C to give 1,3-diphenyltriazoliumfullerene salt $3^+{\cdot}PF_6^-$ (Scheme 1). The ^{13}C-NMR measurement showed *ca.* 16 peaks of sp^2-fullerene carbons (and 4 phenyl peaks, Fig. S1 in the ESI†) and one sp^3 peak at 91 ppm, indicating the occurrence of C_{2v} symmetric addition at the 6,6-bond of fullerene. The downfield shift of the sp^3 carbon is probably because of the electron-withdrawal by the conjunct positive N_1 and N_2 atoms, which is in conformity with a computational simulation (96 ppm by a GIAO/B3LYP/6-31G(d) approach with IEFPCM/DMSO, Fig. S2 in the ESI†). Unfortunately, however, such C_{2v} peaks gradually disappeared with the addition of D_2O into the NMR DMSO solution (*ca.* 10% v/v), while the addition of methanol-d_4 brought about no change in the spectra. This water degradation may be ascribed to the lower LUMO level of triazoliumfullerene (*vs.* water persistent pyrrolidiniumfullerene), which would enhance the electrophilic activity.

The enhancement of the electron accepting ability of 3^+ was also confirmed by cyclic voltammetry (Fig. S3, ESI†). The higher reducing potential of 3^+ (*vs. N,N*-dimethylpyrrolidiniumfullerene[1b,2]) is ascribed to the lower LUMO level due to the periconjugation. The irreversibility of the first peak may indicate the instability of the reduced intermediate. This higher electron accepting ability would lead to intensified n-type semiconductibility and π-soft Lewis acidity.[12] Moreover, 3^+ seems to be a potential candidate for photoinduced electron-transfer materials if some donating counteranions or substituents are introduced.

Although the [3+2] cycloaddition of 1,3-diaza-2-azoniaallene salt with small alkenes was reported to proceed *via* a concerted pathway,[9d,13] it is unclear whether this is also the case for the highly conjugated and strained alkenes like fullerenes. As indicated by DFT calculations[10] (BHandHLYP/6-31G(d) with IEFPCM (toluene)),[13] the unusually low LUMO level (−3.72 eV) of 2^+ is suitable for orbital interaction with the symmetry allowed HOMO (−6.76 eV) of C_{60} (Fig. 2a and b). TS calculations clarified a concerted transition state with the extremely small activation energy of 1.4 kcal mol^{-1} (Fig. 2c and d) and almost equivalent C_{60}–N distances (2.3963 and 2.3965 Å). Moreover, the calculation for the product 3^+ (Fig. S4 in the ESI†) showed a *ca.* 1.0 eV lower HOMO level (−7.79 eV) than that of C_{60}, explaining the absence of bisadducts of 2^+.[14] These theoretical

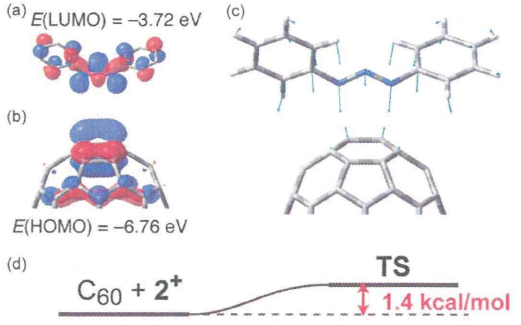

Fig. 2 (a) LUMO of 2^+ (hydrogen omitted), (b) HOMO (in part) of C_{60}, (c) transition state (TS) geometry and the vibrational vectors of imaginary frequency (ν_i = −102.3 cm^{-1}), and (d) energy diagram (ZPE corrected) of the reaction. These calculations were carried out with the BHandHLYP/6-31G(d) level of theory with solvent parameters (IEFPCM, toluene).[13]

results imply that the present [3+2] reaction of 2^+ proceeds *via* a concerted process like 1,3-dipolar cycloaddition, although such HOMO controlled reactions of C_{60} are very rare on account of the inherent low LUMO level of fullerene.[15]

The self-assembly of triazoliumfullerene was assessed by dynamic light scattering (DLS) and scanning and transmission electron microscopy (SEM and TEM). The solvation of its PF_6 salt in THF showed slight aggregation (1×10^{-5} M, *ca.* 100 nm particle size, Fig. 3a). After casting of the solution on a Si-plate and evaporation, SEM images indicated both spherical and nanocrystalline self-assemblies (Fig. 3b and Fig. S5a, ESI†). For the solution with methanol, the ratio of nanocrystals/vesicles

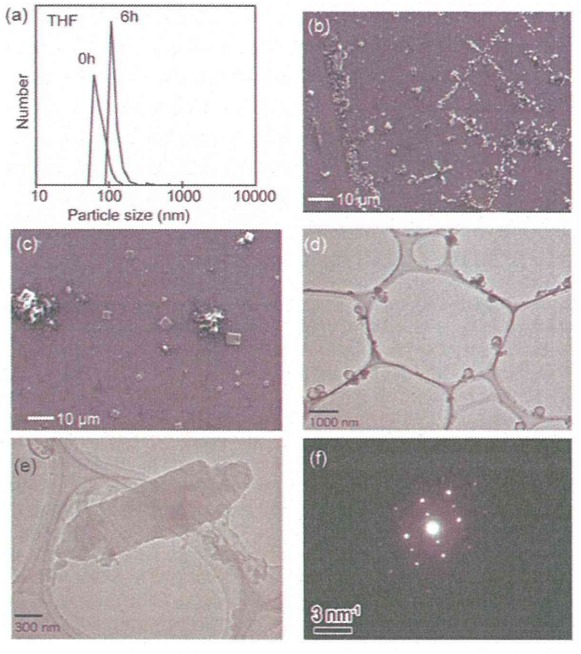

Fig. 3 Aggregation behaviour of $3^+{\cdot}PF_6^-$ salt. (a) DLS measurement in THF solution. SEM image after casting (b) THF solution or (c) MeOH solution. (d) Vesicle and (e) microcrystal TEM images and (f) diffraction pattern after casting MeOH solution on a carbon/Cu microgrid.

seems to increase (Fig. 3c). By TEM analysis, these spherical aggregates seem to be 100–300 nm vesicles with hollow centers (Fig. 3d and Fig. S5b, ESI†), although the present experiments cannot unambiguously certify bilayer formation. Such vesicles have often been observed in ionic fullerenes.[2,3] Interestingly, TEM also showed micrometer-scale crystals (Fig. 3e) with a clear diffraction pattern (Fig. 3f). Such microcrystals were occasionally observed in non-ionic supramolecular fullerenes with semiconductivity.[16] Crystalline triazoliumfullerene can be useful for electron-transport materials with lower LUMO levels, although the configurational control of counteranions is required to inhibit the possible carrier-trapping.

Although the quantitative evaluation of periconjugative effects requires further experiments (*e.g.*, with varying substituents and counteranions), we consider that the moderate amphiphilicity of $\mathbf{3}^+$ with a small dipole moment (~11 D) and highly delocalized positive charge would be responsible for the simultaneous formation of vesicles and microcrystals. While pyrrolidiniumfullerene with a larger dipole (~18 D) preferably aggregates in an antiparallel manner to form bilayers,[1i] the smaller dipole of triazoliumfullerene can exhibit another type of aggregation mode. In this case, the enhanced π-acceptor ability caused by the delocalized positive charge on the fullerene sphere may promote crystalline aggregation with the aid of counteranions as well as the aryl-substituents.

In conclusion, we first prepared triazoliumfullerene by a one-pot reaction of *in situ* generated 1,3-diaza-2-azoniaallene with C_{60} and confirmed the periconjugative delocalization of positive charge into the fullerene cage. This compound is expected to exhibit vesicle/crystalline self-assembly due to its moderate amphiphilic interactions and highly delocalized positive charge.

TEM measurements were carried out by using a piece of equipment in the Research Center for Ultrahigh Voltage Electron Microscopy, Osaka University. We thank Prof. Mikiji Miyata and Dr Ichiro Hisaki for the DLS measurements, Prof. Shu Seki for the SEM measurements, and Dr Keita Kobayashi for the TEM measurements. This work was partly supported by a Grant-in-Aid for Young Scientist (B) (No. 24750039) from JSPS and by Health Labour Sciences Research Grants from MHLW.

Notes and references

1 (*a*) R. Bullard-Dillard, K. E. Creek, W. A. Scrivens and J. M. Tour, *Bioorg. Chem.*, 1996, **24**, 376; (*b*) D. M. Guldi, H. Hungerbuhler and K. D. Asmus, *J. Phys. Chem. A*, 1997, **101**, 1783; (*c*) A. M. Cassell, W. A. Scrivens and J. M. Tour, *Angew. Chem., Int. Ed.*, 1998, **37**, 1528; (*d*) K. Kordatos, T. Da Ros, S. Bosi, E. Vázquez, M. Bergamin, C. Cusan, F. Pellarini, V. Tomberli, B. Baiti, D. Pantarotto, V. Georgakilas, G. Spalluto and M. Prato, *J. Org. Chem.*, 2001, **66**, 4915; (*e*) S. Bosi, L. Feruglio, D. Milic and M. Prato, *Eur. J. Org. Chem.*, 2003, 4741; (*f*) T. Mashino, D. Nishikawa, K. Takahashi, N. Usui, T. Yamori, M. Seki, T. Endo and M. Mochizuki, *Bioorg. Med. Chem. Lett.*, 2003, **13**, 4395; (*g*) S. Bosi, T. Da Ros, G. Spalluto, J. Balzarini and M. Prato, *Bioorg. Med. Chem. Lett.*, 2003, **13**, 4437; (*h*) D. M. Guldi, F. Zerbetto, V. Georgakilas and M. Prato, *Acc. Chem. Res.*, 2005, **38**, 38; (*i*) C. J. Chancellor, A. A. Thorn, C. M. Beavers, M. M. Olmstead and A. L. Balch, *Cryst. Growth Des.*, 2008, **8**, 976.

2 (*a*) A. M. Cassell, C. L. Asplund and J. M. Tour, *Angew. Chem., Int. Ed.*, 1999, **38**, 2403; (*b*) V. Georgakilas, F. Pellarini, M. Prato, D. M. Guldi, M. Melle-Franco and F. Zerbetto, *Proc. Natl. Acad. Sci. U. S. A.*, 2002, **99**, 5075.

3 (*a*) S. Zhou, C. Burger, B. Chu, M. Sawamura, N. Nagahama, M. Toganoh, U. E. Hackler, H. Isobe and E. Nakamura, *Science*, 2001, **291**, 1944–1947; (*b*) H. Isobe, T. Homma and E. Nakamura, *Proc. Natl. Acad. Sci. U. S. A.*, 2007, **104**, 14895.

4 P. Brough, D. Bonifazi and M. Prato, *Tetrahedron*, 2006, **62**, 2110.

5 (*a*) T. Shiga and T. Motohiro, *Thin Solid Films*, 2007, **515**, 3607; (*b*) K. Masuda, T. Abe, H. Benten, H. Ohkita and S. Ito, *Langmuir*, 2010, **26**, 13472; (*c*) H. Li, M. J. Hollamby, T. Seki, S. Yagai, H. Möhwald and T. Nakanishi, *Langmuir*, 2011, **27**, 7493.

6 (*a*) J. C. Hummelen, B. Knight, J. Pavlovich, R. Gonzalez and F. Wudl, *Science*, 1995, **269**, 1554; (*b*) K. C. Kim, F. Hauke, A. Hirsch, P. D. W. Boyd, E. Carter, R. S. Armstrong, P. A. Lay and C. A. Reed, *J. Am. Chem. Soc.*, 2003, **125**, 4024; (*c*) O. Vostrowsky and A. Hirsch, *Chem. Rev.*, 2006, **106**, 5191.

7 Azafullerene is easily reduced to form a dimer, which is a reactive intermediate for further reactions. See (*a*) M. Keshavarz-K, R. Gonzalez, R. G. Hicks, G. Srdanov, V. I. Srdanov, T. G. Collins, J. C. Hummelen, C. Bellavia-Lund, J. Pavlovich, F. Wudl and K. Holczer, *Nature*, 1996, **383**, 147; (*b*) N. B. Shustova, I. V. Kuvychko, A. A. Popov, M. von Delius, L. Dunsch, O. P. Anderson, A. Hirsch, S. H. Strauss and O. V. Boltalina, *Angew. Chem., Int. Ed.*, 2011, **50**, 5537.

8 (*a*) M. Eiermann, R. C. Haddon, B. Knight, Q. C. Li, M. Maggini, N. Martín, T. Ohno, M. Prato, T. Suzuki and F. Wudl, *Angew. Chem., Int. Ed. Engl.*, 1995, **34**, 1591; (*b*) B. Knight, N. Martín, T. Ohno, E. Ortí, C. Rovira, J. Veciana, J. Vidal-Gancedo, P. Viruela, R. Viruela and F. Wudl, *J. Am. Chem. Soc.*, 1997, **119**, 9871; (*c*) P. Ceroni, F. Conti, C. Corvaja, M. Maggini, F. Paolucci, S. Roffia, G. Scorrano and A. Toffoletti, *J. Phys. Chem. A*, 2000, **104**, 156; (*d*) F. B. Kooistra, T. M. Leuning, E. Maroto-Martinez and J. C. Hummelen, *Chem. Commun.*, 2010, **46**, 2097.

9 (*a*) W. Wirschun and J. C. Jochims, *Synthesis*, 1997, 233; (*b*) W. Wirschun, G. M. Maier and J. C. Jochims, *Tetrahedron*, 1997, **53**, 5755; (*c*) W. Wirschun, M. Winkler, K. Lutz and J. C. Jochims, *J. Chem. Soc., Perkin Trans. 1*, 1998, 1755; (*d*) M. Weng, A. Geyer, A. Friemel, J. C. Jochims and M. Lutz, *J. Prakt. Chem.*, 2000, **342**, 486.

10 In this paper, all DFT calculations were carried out with Spartan'08 or Gaussian 09. Full citations are shown in the ESI.†.

11 J. Bouffard, B. K. Keitz, R. Tonner, G. Guisado-Barrios, G. Frenking, R. H. Grubbs and G. Bertrand, *Organometallics*, 2011, **30**, 2617. Attempts to obtain a $SbCl_6^-$ salt (see ref. 9) failed probably because of the occurrence of chlorination of C_{60} by $SbCl_5$.

12 (*a*) H. Li, C. Risko, J. H. Seo, C. Campbell, G. Wu, J.-L. Brédas and G. C. Bazan, *J. Am. Chem. Soc.*, 2011, **133**, 12410; (*b*) J. Iglesias-Sigüenza and M. Alcarazo, *Angew. Chem., Int. Ed.*, 2012, **51**, 1523.

13 S. Y. Yang, X. F. Lin, C. K. Sun and D. C. Fang, *THEOCHEM*, 2007, **815**, 127. Our calculation used a rather simplified BHandHLYP/6-31G(d) method to reduce its calculational cost.

14 However, the use of a large excess of **1** and KPF_6 gave inseparable byproducts, *e.g.*, bi- and multi-adducts or products due to the decomposition of the labile intermediate $\mathbf{2}^+$.

15 Most 1,3-dipoar reactions of fullerene proceed with nucleophiles rather than electrophiles, except for the addition of ozone. See (*a*) R. Malhotra, S. Kumar and A. Satyam, *J. Chem. Soc., Chem. Commun.*, 1994, 1339; (*b*) D. Heymann, S. M. Bachilo, R. B. Weisman, F. Cataldo, R. H. Fokkens, N. M. M. Nibbering, R. D. Vis and L. P. F. Chibante, *J. Am. Chem. Soc.*, 2000, **122**, 11473.

16 (*a*) X. Zhang and M. Takeuchi, *Angew. Chem., Int. Ed.*, 2009, **48**, 9646; (*b*) X. Zhang, T. Nakanishi, T. Ogawa, A. Saeki, S. Seki, Y. Shen, Y. Yamauchi and M. Takeuchi, *Chem. Commun.*, 2010, **46**, 8752; (*c*) T. Nakanishi, Y. Shen, J. Wang, H. Li, P. Fernandes, K. Yoshida, S. Yagai, M. Takeuchi, K. Ariga and D. G. Kurth, *et al.*, *J. Mater. Chem.*, 2010, **20**, 1253; (*d*) S. S. Babu, H. Möhwald and T. Nakanishi, *Chem. Soc. Rev.*, 2010, **39**, 4021; (*e*) S. Santhosh Babu, A. Saeki, S. Seki, H. Möhwald and T. Nakanishi, *Phys. Chem. Chem. Phys.*, 2011, **13**, 4830.

CARBON 68 (2014) 346–351

Available at www.sciencedirect.com

ScienceDirect

journal homepage: www.elsevier.com/locate/carbon

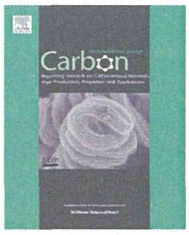

Effect of functional group polarity on the encapsulation of C_{60} derivatives in the inner space of carbon nanohorns

Keita Kobayashi [a,*], *Hiroshi Ueno* [b], *Ken Kokubo* [b], *Masako Yudasaka* [c], *Hidehiro Yasuda* [a]

[a] *Research Center for Ultra-High Voltage Electron Microscopy, Osaka University, 7-1, Mihogaoka, Ibaraki, Osaka 567-0047, Japan*
[b] *Division of Applied Chemistry, Graduate School of Engineering, Osaka University, 2-1, Yamadaoka, Suita, Osaka 565-0871, Japan*
[c] *Nanotube Research Center, National Institute of Advanced Industrial Science and Technology (AIST), 1-1-1, Higashi, Tsukuba 305-8565, Japan*

ARTICLE INFO

Article history:
Received 30 August 2013
Accepted 6 November 2013
Available online 13 November 2013

ABSTRACT

Encapsulation of C_{60}, its hydroxides ($C_{60}(OH)_n$, $n = 10$, 36, 44), and its hydride ($C_{60}H_{36}$) into inner space of carbon nanohorns (CNHs) from solutions or dispersions in various solvents by the nano-condensation method was attempted. The effect of the functional groups on the encapsulation was evaluated by transmission electron microscopy. C_{60}, $C_{60}(OH)_{10}$, and $C_{60}H_{36}$ can be efficiently encapsulated inside CNHs using toluene, THF, and DMSO as solvents, whereas $C_{60}(OH)_{36}$ and $C_{60}(OH)_{44}$ are hardly encapsulated from any solution. Because the molecular size of $C_{60}(OH)_{10}$ is similar to that of $C_{60}(OH)_{36}$ and $C_{60}(OH)_{44}$, the difference in encapsulation is not caused by molecular size. The efficient encapsulation of $C_{60}H_{36}$ in CNHs suggests that molecules can be encapsulated in carbon nanomaterials even when the π–π interaction with the sp^2-hybridized carbon walls is weak. These results suggest the polarity of the functional group of the C_{60} derivatives as the main factor in determining whether they can be encapsulated in CNHs. $C_{60}(OH)_{36}$ and $C_{60}(OH)_{44}$ contain many hydroxyl groups, thus these molecules self-aggregate and do not pass the holes of CNHs, resulting in poor encapsulation.

1. Introduction

A single C_{60} molecule encapsulated in a carbon nanotube (CNT) or a carbon nanohorn (CNH) can be distinguished by transmission electron microscopy (TEM) because of its unique molecule shape [1–5]. Since inner space of CNTs and CNHs can encapsulate other molecules, these tubular carbon nanomaterials have been widely used as nano test tubes for observing molecule structures and behaviours by TEM [1–13] and other methods (Raman [11–13] and electron spin resonance spectroscopy [12,14]). Especially, the direct TEM observation of individual molecules is a powerful method for understanding molecular structure and behaviour. Observation of isolate organic molecules encapsulated in inner space of tubular carbon nanomaterials is still problematic, because it is difficult to distinguish the objective molecules from contaminants in the TEM specimen. The unique molecular shape of C_{60} can be identified by TEM, therefore, the organic molecules covalently bond to C_{60} also can be observed with TEM. This technique has been used to observe the unique structure and behavior of molecules [6–11].

Functionalization of C_{60} with the organic molecules changes the electronic state and polarity of C_{60}. Although C_{60} can be efficiently encapsulated into the inner space of

* *Corresponding author:* Fax: +81 6 6879 7942.
E-mail address: kobayashi-z@uhvem.osaka-u.ac.jp (K. Kobayash.
0008-6223/$ - see front matter © 2013 Elsevier Ltd. All rights reserved.
http://dx.doi.org/10.1016/j.carbon.2013.11.011

tubular carbon nanomaterials through of the π–π interaction [15,16], functionalization may prevent encapsulation. Therefore, it is important to clarify the effect of functionalization on the encapsulation of C_{60} derivatives in tubular carbon nanomaterials.

In this study, we encapsulated pristine C_{60} fullerene, its hydroxides ($C_{60}(OH)_n$, $n = 10$, 36, 44), and its hydride ($C_{60}H_{36}$) in the inner space of CNHs from solutions or dispersions of various solvents by the nano-condensation method [4]. The effect of the functional groups on the encapsulation of these molecules was evaluated by TEM observations and electron energy loss spectroscopy (EELS).

2. Experimental

$C_{60}(OH)_{36}$ and $C_{60}(OH)_{44}$ were synthesized from $C_{60}(OH)_{10}$ (Frontier Carbon Corporation) and C_{60} (American Dye Source, 99.5%), respectively, using previously reported procedures [17–20].

CNH aggregates (NEC, 90%, produced by laser-vaporization of a graphite target [21,22]) were heat-treated at 853 K for 10 min under air to remove amorphous carbon impurities and to open paths to the internal space [5]. The heat-treated CNH aggregates were dispersed in methanol (Kishida Chemical, 99.8%) using bath-type ultrasonicator (Honda Electronics, W-103T). Then the CNH aggregates were suspended on a TEM microgrid (Oken Shoji, STEM150Cu B-type) by dropping the suspension onto the microgrid.

To encapsulate C_{60} or C_{60} hydroxides into the CNHs, 1 mg of these molecules were solved or dispersed into 3 ml of solvents: a toluene (Wako Pure Chemical Industries (Wako), 99.8%), a tetrahydrofuran (THF; Wako, 99.5%), or a dimethyl sulfoxide (DMSO; Wako, 99%). Solubility and size distributions of the solved or dispersed molecules in the solvents were measured by dynamic light scattering (DLS; Otsuka Electronics, FPAR-1000HR) (shown in the Supplementary data). These solutions or dispersions were dropped onto the TEM microgrid suspending the CNHs (nano-condensation method [4]). Additionally, $C_{60}H_{36}$ (Frontier Carbon Corporation) was also encapsulated into the CNHs by the nano-condensation method in THF or toluene solution.

The chemical structures of C_{60} and its derivatives were evaluated by Fourier transform infrared spectroscopy (FT-IR; JASCO, FT/IR-410). The morphological structures of the molecules encapsulated within CNHs were also observed by an atomic resolution analytical TEM (JEOL, JEM-ARM200F/UHR) operating at 120 kV. The electronic states of C_{60} and its derivatives were evaluated by EELS of their powder, which were prepared dispersing in a toluene and suspending on a TEM microgrid, using a post-column TEM energy filter (Gatan, GIF Quantum) mounted on the TEM system.

3. Results and discussion

First, we confirmed the structure of fullerenes. Fig. 1a shows a photograph of powdered samples of C_{60}, its hydroxides, and the hydride. The colors of these powders indicate that the complementary colors of the powders are blue-shifted as the number of hydroxyl groups increases. This suggests that

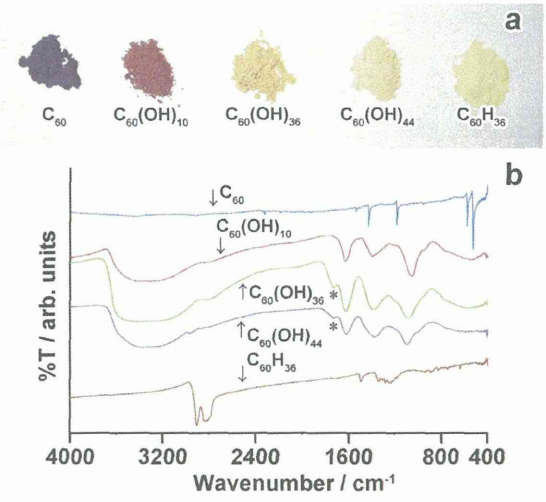

Fig. 1 – (a) Photograph and (b) IR spectra of C_{60}, $C_{60}(OH)_n$ ($n = 10$, 36, and 44), and $C_{60}H_{36}$.

$C_{60}(OH)_{36}$ and $C_{60}(OH)_{44}$ are almost transparent to visible light because of the considerable decrease in π-conjugation [17]. Similarly, the color of $C_{60}H_{36}$ indicates that its sp^2 character is as small as that of $C_{60}(OH)_{36}$ and $C_{60}(OH)_{44}$. The IR spectra of C_{60}, $C_{60}(OH)_{10}$, $C_{60}(OH)_{36}$, $C_{60}(OH)_{44}$, and $C_{60}H_{36}$ are shown in Fig. 1b. The IR spectrum of C_{60} contains four sharp absorption peaks at 528, 577, 1183, and 1429 cm^{-1}. These peaks are attributed to the F_{1u} vibration modes of C_{60} and indicate its icosahedral symmetry [23,24]. The IR spectra of $C_{60}(OH)_{10}$, $C_{60}(OH)_{36}$, and $C_{60}(OH)_{44}$ show substantially different spectral patterns from that of C_{60}, and contain broad absorption peaks at 1080, 1370, 1620, and 3400 cm^{-1} which can be assigned to νC–O, δ_sC–O–H, νC=C, and νO–H, respectively [18]. The relative absorption intensity of the absorption band at 3400 nm^{-1} in the spectra increase in the order $C_{60}(OH)_{10}$, $C_{60}(OH)_{36}$, and $C_{60}(OH)_{44}$, corresponding to the increase in the number of hydroxyl groups. In the $C_{60}(OH)_{36}$ and $C_{60}(OH)_{44}$ spectra, an additional small peak at 1720 cm^{-1} (denoted by asterisks) can be assigned to a carboxyl group formed by the further oxidation of a hydroxyl group associated with C–C bond cleavage of the fullerene cage, or to a carbonyl group formed by the pinacol rearrangement of a vicinal hydroxyl group in fullerene [17,25,26]. Although the IR spectra indicate that the actual chemical abundances of $C_{60}(OH)_{36}$ and $C_{60}(OH)_{44}$ deviate slightly from the ideal stoichiometry, they confirms that these molecules are well hydroxylated. The IR spectrum of $C_{60}H_{36}$ shows weak bands at 1100–1400 cm^{-1}, one weak peak at ~1493 cm^{-1}, and two peaks at ~2830 and ~2905 cm^{-1}. These peaks are assigned to δC–C–H vibrations, aromatic ring vibrations, and νC–H vibrations, respectively, and they suggest that the molecule is properly hydrogenated [27].

The electron states were further confirmed by EELS. EELS in the region of the carbon K-shell excitation of C_{60} and its hydroxides are shown in Fig. 2. The C_{60} spectrum shows a band at around 280–287 eV and a shoulder peak at 288.3 eV, which are assigned to the 1s $\rightarrow \pi^*$ transition [28–30], and the two bands at 292 and 300 eV are assigned to the 1s $\rightarrow \sigma^*$